Eur. Phys. J. C (2025) 85:870
https://doi.org/10.1140/epjc/s10052-025-14595-y

THE EUROPEAN PHYSICAL JOURNAL C

Regular Article - Theoretical Physics

A parton shower consistent with parton densities at LO and NLO: PDF2ISR

H. Jung[1,2,a], **L. Lönnblad**[3,b], **M. Mendizabal**[1,c], **Sara Taheri Monfared**[1,d]

[1] Deutsches Elektronen-Synchrotron DESY, Hamburg, Germany
[2] II. Institut für Theoretische Physik, Universität Hamburg, Hamburg, Germany
[3] Department of Physics, Lund University, Lund, Sweden

Received: 17 April 2025 / Accepted: 29 July 2025

Abstract We present a method for obtaining an initial-state parton shower model where the (backward) evolution fully consistent with the (forward) evolution of the collinear parton density used. As a proof-of-concept we use parton densities obtained with the parton branching (PB) approach, and modify the default initial-state shower in PYTHIA8 with this method to be consistent with them. PB is ideally suited for checking the validity of our method since, in addition to producing collinear parton densities, it also produces the corresponding transverse-dependent (TMD) ones, and these can then be directly compared to the transverse momentum distribution obtained from the parton shower. We show that TMD distributions which we in this way obtain from our modified PYTHIA8 shower using leading order (LO) parton densities and splitting functions are fully consistent with the corresponding leading order TMD densities. At next-to-leading order (NLO) it is not possible to achieve the same consistency using the built-in LO splitting functions in the shower, but we show that by introducing NLO splitting functions using a reweighting procedure, we can achieve consistency also at NLO. The method presented here, which we have named PDF2ISR, can be easily extended to any collinear parton densities, as long as the exact conditions for the evolution are known. With the PDF2ISR method we obtain an initial-state parton shower which in principle has no free parameters, and is fully consistent with collinear parton densities at LO and NLO.

1 Introduction

The description of precise measurements of processes involving high transverse momentum jets as well as precision measurements of vector-boson production require rather sophisticated methods. Only in rare cases a description using fixed-order perturbative calculations is sufficient. In most cases, a simulation, including multiple partonic radiation and hadronization, as performed in multi-purpose Monte Carlo event generators (MCEG) like HERWIG [1], PYTHIA8 [2], and SHERPA [3,4], is required.

The hard, perturbative process can be calculated externally via packages like MADGRAPH5_AMC@NLO [5] or POWHEG [6,7] at leading-order (LO) or next-to-leading order (NLO) accuracy, and can be supplemented with initial- and final-state parton showers, as well as with multi-parton interactions and hadronization. While quite some effort has been put into matching and merging of parton showers with the NLO matrix element calculations [5,8–12], parton showers still appear to lack a direct correspondence with the parton densities used in the calculation of the hard process as well as in the backward evolution. In Ref. [13], it is argued that collinear parton densities, as well as NLO hard scattering coefficients, must be recalculated in a scheme that corresponds to the one used in parton showers, pointing to an inconsistency in the present treatment.

In this paper we describe a method, called PDF2ISR, to construct the initial-state radiation (ISR) simulated as a parton shower to follow exactly the evolution of the collinear parton density by using the parton-branching (PB)-method [14,15] as a test-case. The PB-approach has been developed as a method to solve the evolution equations iteratively, in order to provide collinear as well as transverse momentum dependent (TMD) parton densities, by simulating each individual branching and including the appropriate kinematic relations.

[a] e-mail: hannes.jung@desy.de (corresponding author)
[b] e-mail: leif.lonnblad@fysik.lu.se
[c] e-mail: mikel.mendizabal.morentin@desy.de
[d] e-mail: sara.taheri.monfared@desy.de

Published online: 12 August 2025

TMD parton densities are ideal for testing the consistency of the evolution and the parton shower, since they can be obtained from both. The advantage of the PB method is that all the details of each individual branching processes are known and can be studied. The PB-TMD distributions agree by construction with the collinear distribution upon integrating over the transverse momentum exactly. In order to obtain PB-TMD distributions the evolution scale is interpreted as a physical scale with a relation to the transverse momentum of the emitted parton.

In this study, we modify the default.[1] initial-state parton shower in PYTHIA8 to use the parameters of the collinear PB parton distribution and to follow the same kinematic constraints as in the parton evolution to obtain effective TMD distributions. We find that only minor modifications of the PYTHIA8 code are needed to obtain TMD distributions that are in perfect agreement with those from PB at LO. This illustrates and proves that the same physical picture is being used. Going to NLO collinear parton densities, we show that the use of LO splitting functions leads to inconsistent results, and the implementation of NLO splitting functions into the initial-state radiation framework is required. We apply a method, described in Refs. [16,17] to properly treat negative contributions of NLO splitting functions at large z (and small k_t) within a parton shower framework.

In the following, we briefly describe a method to obtain TMD distributions from general parton shower event generators. We will then apply this method to compare the TMD distributions obtained from PB with those from PYTHIA8. We will then describe how the parton shower in PYTHIA8 can be modified to follow the same conditions as those used in PB-method at LO. We discuss in detail the use of collinear parton densities obtained at NLO and show the importance of applying NLO splitting functions, as well as the same evolution method for α_s at NLO. We comment on the frame dependence in the calculation of the transverse momentumk_t in the TMDs.

2 TMDs from parton showers: PS2TMD-method

In a parton shower approach, each individual branching process is simulated using appropriate kinematics (for the notation see Fig. 1).

Due to the kinematic relations in each splitting, a transverse momentum of the emitted parton c as well as of the partons a and b will appear. After the full initial-state shower is generated, an effective final transverse momentum distribution can be reconstructed.

[1] There are several showers implemented in PYTHIA8, the default one is called `SimpleSpaceShower`.

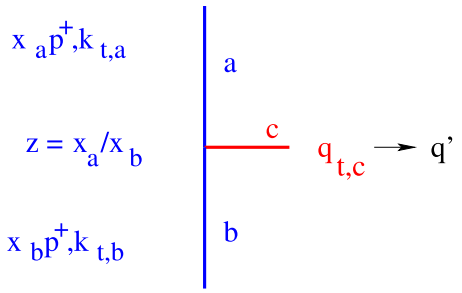

Fig. 1 Typical parton branching process $b \to a + c$

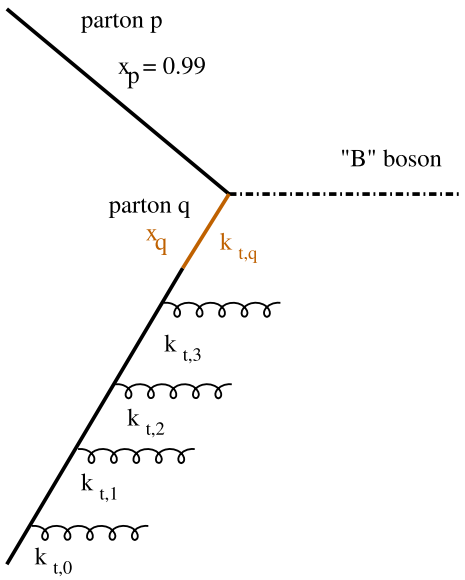

Fig. 2 Illustration of the toy process: $p + q \to B$: (left) bare process; (right) including initial-state parton shower

This effective TMD distribution can be obtained from any parton shower MCEG with the PS2TMD-method [18,19] (see Fig. 2): A toy $2 \to 1$ process ($p + q \to B$) is generated, where one initial parton has momentum fraction $x_p = 0.99$ and does not develop any initial-state radiation, while the other parton has varying x_q according to the collinear parton density and can develop an initial-state parton shower. The produced toy colorless "B-boson" particle is used to calculate the kinematics and for easy identification in the event record. The B-boson can couple equally to gluons and quarks and is therefore unphysical. The scale μ of the process is generated over a large range. The transverse momentum of the initial parton q is easily obtained from the kinematics of the process:

$$k_{t,q} = p_{t,B} \tag{1}$$

with $p_{t,B}$ being the transverse momentum of the particle B (the transverse momentum of parton p is negligible by construction). The cross section of the toy process consists

only of the momentum weighted collinear parton density, at the generated x_q and the scale μ. The generated events are passed to a Rivet plugin [20], where the momentum fraction x_q, the scale μ as well as the transverse momentum $k_{t,q}$ are extracted. Their values are then stored in a grid to be directly used within TMDLIB [21] and visualized with TMDPLOTTER.

The PS2TMD-method has already been validated using CASCADE3 [22] and applied to PYTHIA8 and HERWIG [18,19].

3 PB-method and PYTHIA8 parton shower

We start with a short summary of the main features of the PB-method, followed by a description of the different ordering conditions and brief overview of the PYTHIA8 parton shower method. We then compare TMD distributions obtained with the PB-method to those from the PYTHIA8 initial-state parton shower.

3.1 PB-method

The DGLAP evolution equation [23–26] for the momentum-weighted parton density $xf_a(x,\mu^2)$ of parton a with momentum fraction x at scale μ is written as:

$$\mu^2 \frac{\partial(xf_a(x,\mu^2))}{\partial\mu^2} = \sum_b \int_x^1 dz\ P_{ab}(z,\alpha_s)\ \frac{x}{z} f_b\left(\frac{x}{z},\mu^2\right), \tag{2}$$

where P_{ab} represents the regularized DGLAP splitting functions, describing the transition of parton b into parton a.

After replacing the plus-prescription in P_{ab} with a Sudakov form factor, Δ_a, the solution of the evolution equation for momentum-weighted parton densities, $xf_a(x,\mu^2)$, at scale μ can be written as (e.g. [27]):

$$xf_a(x,\mu^2) = \Delta_a(\mu^2) xf_a(x,\mu_0^2) + \sum_b \int_{\mu_0^2}^{\mu^2} \frac{dq'^2}{q'^2} \frac{\Delta_a(\mu^2)}{\Delta_a(q'^2)} \times \int_x^{z_M} dz\ P_{ab}^{(R)}(z,\alpha_s) \frac{x}{z} f_b\left(\frac{x}{z},q'^2\right), \tag{3}$$

where $P^{(R)}$ are the real, unregularized splitting functions,[2] μ_0 is the starting scale, $\Delta_a(\mu^2) := \Delta_a(\mu^2,\mu_0^2)$ is the Sudakov form factor and $\mathbf{q}'$ is a 2-dimensional vector with $\mathbf{q}'^2 = q'^2$. From the comparison of Eq. (2) with Eq. (3), one can immediately see that, for consistency, $z_M \to 1$. However, for numerical reasons, $z_M = 1-\epsilon$ with very small ϵ to avoid the $1/(1-z)$ singularity in splitting functions.

The PB approach provides a method to solve the evolution equation by an iterative method, applying the concept of Sudakov form factors, as described in Refs. [14,15]. The advantage of this iterative approach is that each individual splitting process is simulated, allowing for proper treatment of the kinematic relations of the splitting. This method has been applied to determine collinear and TMD distributions by fitting the parameters of the initial distribution [28] such that deep-inelastic measurements at HERA [29] can be well described over a wide range in x and Q^2.

Two different sets were obtained in Ref. [28], depending on the scale choice in α_s: in PB-NLO-2018 Set1 the evolution scale q' was used as the scale in α_s resulting in collinear distributions identical to those obtained as HERAPDF; in PB-NLO-2018 Set2 the transverse momentum q_t (for a definition see next section) was used as the scale in α_s, and different collinear and TMD distributions were obtained, with a similar $\chi^2/ndf \sim 1.2$. This scale choice for α_s is motivated from angular ordering, and leads to two different regions: a perturbative region, with $q_t > q_{cut}$, and a non-perturbative region of $q_t < q_{cut}$, where α_s is frozen at q_0. The initial distributions were defined at a scale $\mu_0 = 1.374(1.181)$ GeV for PB-NLO-2018 Set1(Set2).

3.2 Ordering conditions in PB-method

The DGLAP evolution equations allow the determination of the parton densities at a scale μ if they are known at a different scale μ_0. However, these equations do not provide a physical interpretation of the evolution scale. In parton shower approaches, as well as in the PB-method, the DGLAP equations are extended by giving a physical interpretation to the evolution scale. A typical branching process, $b \to a + c$, is shown in Fig. 1, with the light-cone momenta $p_a^+ = zp_b^+$, $p_c^+ = (1-z)p^+$ with p^+ being the light-cone momentum of the beam particle.

The transverse momentum $q_{t,c}$ can be calculated from the evolution scale μ in different ways:

- p_t-ordering: the transverse momentum $q_{t,c}$ is directly associated with the evolution scale μ, such that $q_{t,c} = q'$
- angular ordering: the rescaled transverse momentum $q_{t,c}/(1-z)$ is related to the polar angle Θ_c of the emitted parton, which is taken as the evolution scale, resulting in $q_{t,c} = (1-z)q'$.

Ref. [15] presents transverse momentum distributions obtained from p_t- and angular ordering, illustrating significant differences between them.

3.3 Initial-state shower in PYTHIA8

The initial-state parton shower in PYTHIA8 starts from the hard scattering using a backward evolution applying ratios

[2] Replacing $1/(1-z)_+$ by $1/(1-z)$ and without the virtual contribution.

of collinear parton densities. A detailed description of the parton shower approach is given in Refs. [2,30].

The probability for an emission is given by the Sudakov form factor for backward evolution:

$$\log \Delta_{bw}(z,\mu,\mu_{i-1}) = -\sum_b \int_{\mu_{i-1}^2}^{\mu^2} \frac{dq'^2}{q'^2} \times \int_x^{z_{\rm dyn}} dz P_{ab}^{(R)}(\alpha_s(z,q'),z) \frac{x' f_b(x',q')}{x f_a(x,q')} \,. \quad (4)$$

By default, the scale q' is the transverse momentum of the emitted parton. Additional corrections are applied for heavy flavoured partons. The default ordering condition in PYTHIA8 is transverse momentum ($p_{\rm t}$-) ordering, implying the evolution scale $q' = p_{\rm t}$. The integration limit $z_{\rm dyn}$ is constrained by the masses of the radiating dipole system, with $z_{\rm dyn} < 1$. In general, $z_{\rm dyn}$ in Eq. (4) does not match $z_{\rm M}$ in Eq. (3).

It should be noted that the splitting probability by default is smoothly suppressed for small transverse momenta by a factor $p_\perp^2/(p_\perp^2 + p_{\perp 0}^2)$, together with a hard cutoff at $p_{\perp\rm min}$.

3.4 PB-TMDs and effective TMDs from PYTHIA8

In the following we compare the predictions from PB Set1 with those obtained from PYTHIA8 initial-state parton shower using parameters from the CUET tune.[3] We apply the PS2TMD-method using PYTHIA8 (version 8.311) to generate the initial-state (space-like) parton shower. The distributions are obtained by running the toy process described in Sect. 2 at $\sqrt{s} = 5 \cdot 10^6$ GeV to ensure appropriate coverage of the phase space.

In Fig. 3 (upper row) we show a comparison of TMD distributions obtained from PB-NLO-2018 Set1 [28] with those from space-like parton showers of PYTHIA8. The distributions differ significantly, as expected, due to the different ordering conditions used. For better comparison between the true parton shower and the PB-evolution, we show the distributions without including any intrinsic-$k_{\rm t}$ contribution in Fig. 3 (lower row).

4 The PDF2ISR method in PYTHIA8

The PDF2ISR method is developed using the PB method with collinear and TMD parton densities, combined with the PYTHIA8 parton shower machinery. The basic ingredients of the PB collinear and TMD parton densities are angular ordering and the choice of the scale in α_s. We reinterpret the evolution scale in PYTHIA8 to be $p_{\perp\rm evol} = p_\perp/(1-z)$ rather than $p_\perp$ (for a technical description see Appendix A) in a way such that the starting scale, μ_0, can be identified with $p_{\perp\rm cut}$ (and setting $p_{\perp 0}^2 = 0$, to avoid the smooth suppression described in Sect. 3.3). The quark masses are chosen according to the PB distributions. A complete list of the parameters used is given in Appendix C.

In Eq. (4), the integral over z is limited by $z_{\rm M}$. In the DGLAP framework, $z_{\rm M} = 1$, whereas in a numerical calculation $z_{\rm M} \neq 1$ due to the presence of $1/(1-z)$ poles in the splitting functions. In parton shower approaches, it is often argued that z is limited by kinematics, and by requiring a minimum transverse momentum of the emitted parton one obtains a limit on $z_{\rm M} < 1$. However, as argued in Ref. [31] (and shown explicitly in Ref. [32] for the case of the $p_{\rm t}$ spectrum of DY pairs) soft gluons with $z \to 1$ play an important role especially in the small $k_{\rm t}$-region. In PB Set1, $z_{\rm M} = 0.99999$ is used, and the same value is also applied in the PYTHIA8 studies presented here.

In order to comply with the treatment of heavy flavors in PB, which follows the Variable Flavor Zero Mass (VFZM) scheme, any special heavy flavor treatment in the PYTHIA8 parton shower has been disabled.

4.1 Effective TMDs from PYTHIA8-PDF2ISR with fixed α_s

We begin by calculating PB collinear and TMD distributions with UPDFEVOLV2 [33] at LO and NLO (keeping all other parameters as in PB-NLO-2018 (Set2) but without intrinsic $k_{\rm t}$-distribution). To specifically focus on the splitting functions, we apply a fixed value of $\alpha_s = 0.13$.

In Fig. 4 we compare the calculations of LO PB-TMD distributions with the one obtained from the PYTHIA8 parton shower applying PDF2ISR for down quarks and gluons at two different scales $\mu = 10(100)$ GeV. The results are in very good agreement, indicating that the PDF2ISR-method successfully reproduces distributions obtained from the PB-method.

We now investigate distributions obtained with NLO PB-TMD distributions. In Fig. 5, a comparison is presented between calculations using UPDFEVOLV2 with NLO splitting functions (in toy mode with fixed α_s) and predictions from the PYTHIA8-PDF2ISR parton shower with standard LO splitting functions (blue lines). Obviously, significant differences in the TMD distribution for quarks are observed, which also illustrates the inconsistency using NLO parton densities with LO splitting functions inside the parton shower.

We have implemented the full NLO splitting functions (taken from QCDnum [34]) to be used in the PYTHIA8-PDF2ISR parton shower. In the ISR simulation only about 0.1% branchings come with negative weights, mainly coming from the region of large z and low $p_{\rm t} < 1$ GeV.[4] The

[3] PYTHIA8 setting: `Tune:pp = 18`.

[4] At this stage we ignore negative parts of the splitting function. The correct treatment will be discussed later.

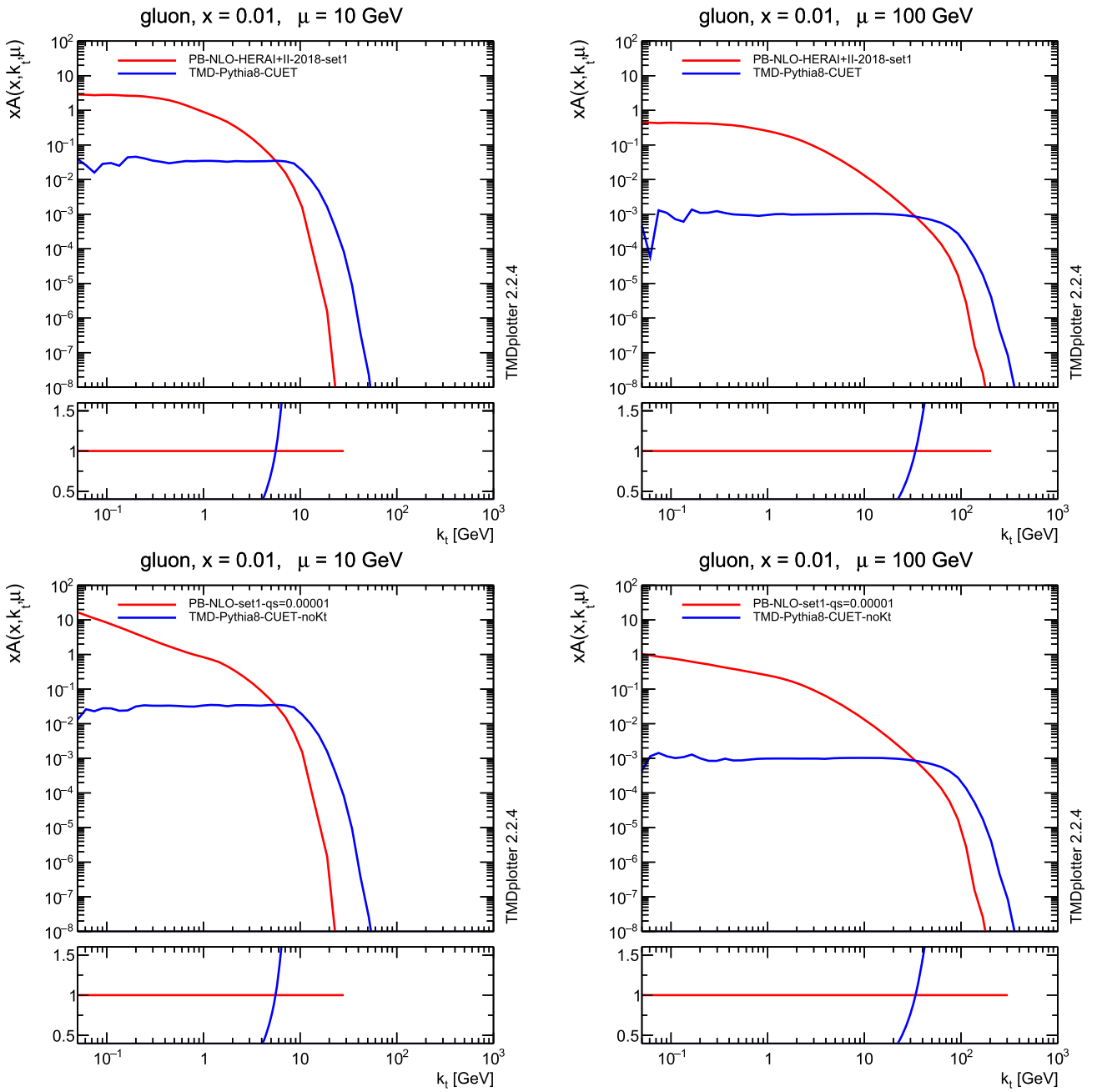

Fig. 3 Transverse momentum distributions for gluons at two different scales $\mu = 10(100)$ GeV (PB-NLO-2018 Set1), obtained from PB-method [28] and PYTHIA8 (CUET tune). The upper row shows the distributions with the intrinsic-k_t distribution, and the lower row shows the distributions without it

purple line in Fig. 5 shows the predictions from the PYTHIA8-PDF2ISR with NLO splitting functions, restricted to channels that also appear at LO (labeled as NLOtrunc).[5] The agreement with the NLO PB-TMD distributions is significantly improved, highlighting the mismatch when different orders of splitting functions are used in the evolution and in the parton shower.

[5] We have explicitly checked and confirmed that the additional channels at NLO have a negligible effect on the TMD distributions.

5 PDF2ISR at NLO

In the previous section we have shown with the toy model that the PYTHIA8-PDF2ISR can reproduce the TMD distributions very well both at LO and NLO provided the corresponding order of splitting functions is applied. We can now discuss predictions obtained with the available PB-NLO-2018 distributions. A comparison with the LO distributions is shown in Appendix D. We use PB-TMD distributions at NLO obtained

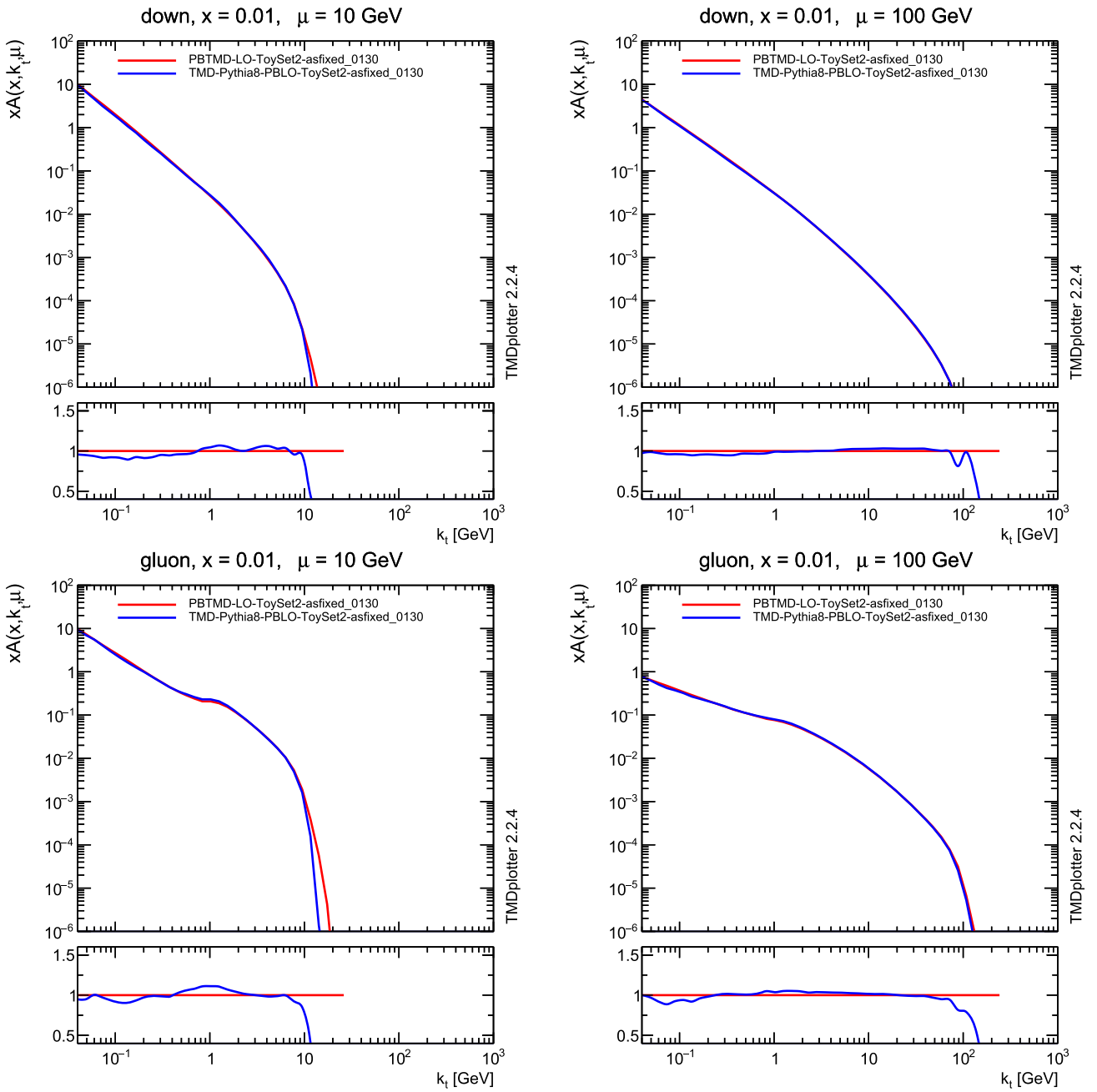

Fig. 4 Transverse momentum distributions for gluons and down-quarks at $\mu = 10(100)$ GeV, obtained from PB-Toy Set2 evolved from a starting scale $\mu_0 = 1.18$ GeV and PYTHIA8 applying angular ordering and `pTmin =1.18` GeV. The predictions are obtained at LO (with fixed $\alpha_s = 0.130$)

in Ref. [28] including an intrinsic-k_t distribution with width $q_s = 0.5$ GeV.

5.1 α_s at NLO

The PB-NLO-2018 distributions were obtained using α_s and the splitting functions as implemented in QCDNUM. While α_s at LO is trivial (provided the same value of Λ_{qcd} and the same mass thresholds are used), differences in the evolution of α_s at NLO show up, depending on which evolution scheme is used. Inside PYTHIA8 the evolution scheme from PDG [35] is applied, while QCDNUM uses a numerical integration instead of a parameterization. Differences between the two approaches are visible especially in the region of low scales, as shown in Fig. 6. Technically, the parametrization which is stored in the LHApdf file will be employed later.

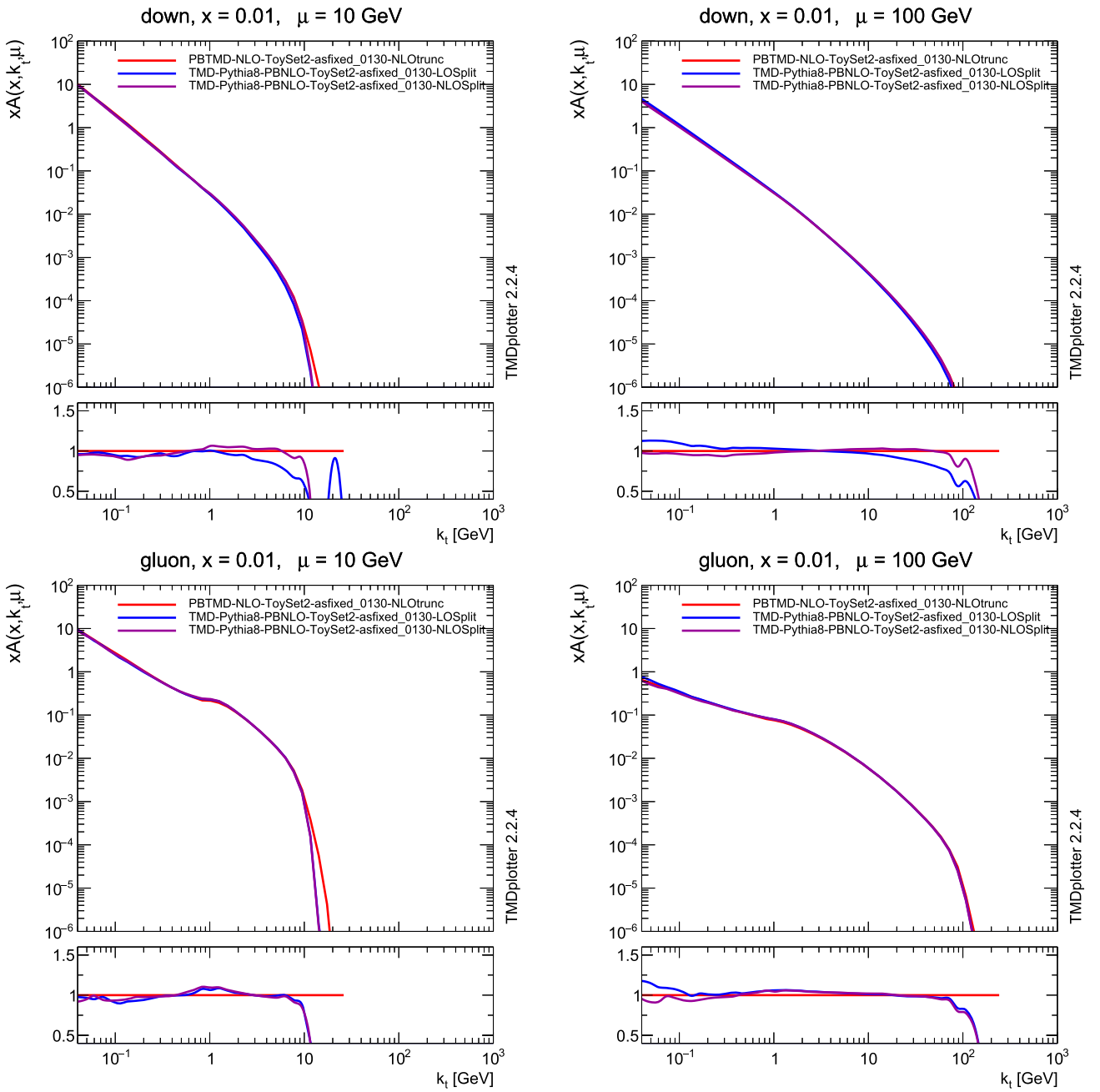

Fig. 5 Transverse momentum distributions for gluons and down-quarks as $\mu = 10(100)$ GeV. The red line is obtained from uPDFevolv2 (PBTMD-ToySet2) evolved from a starting scale $\mu_0 = 1.18$ GeV using NLO splitting functions (for details see text). The predictions using the Pythia8-Pdf2Isr with LO splitting functions are shown in blue, those with NLO splitting functions are shown in purple. In all cases fixed $\alpha_s = 0.130$ is applied

5.2 The treatment of negative contributions in NLO splitting functions

A parton shower simulation is based on probabilities for radiation by interpreting the Sudakov form factor Eq. (4) as a no-emission probability. Technically, the generation is done by the so-called Veto Algorithm, where the splitting functions can be conveniently overestimated in a first step, thus underestimating the no-emission probability, and then applying a veto in a secondary step to obtain not only the correct emission probability but also the correct no-emission probability (see [36]). This interpretation of the Sudakov form factor is, however, only valid for LO splitting function. At NLO, the splitting functions are no longer positive definite, and any interpretation in terms of probabilities is therefore excluded. We can overcome this problem by using LO splitting func-

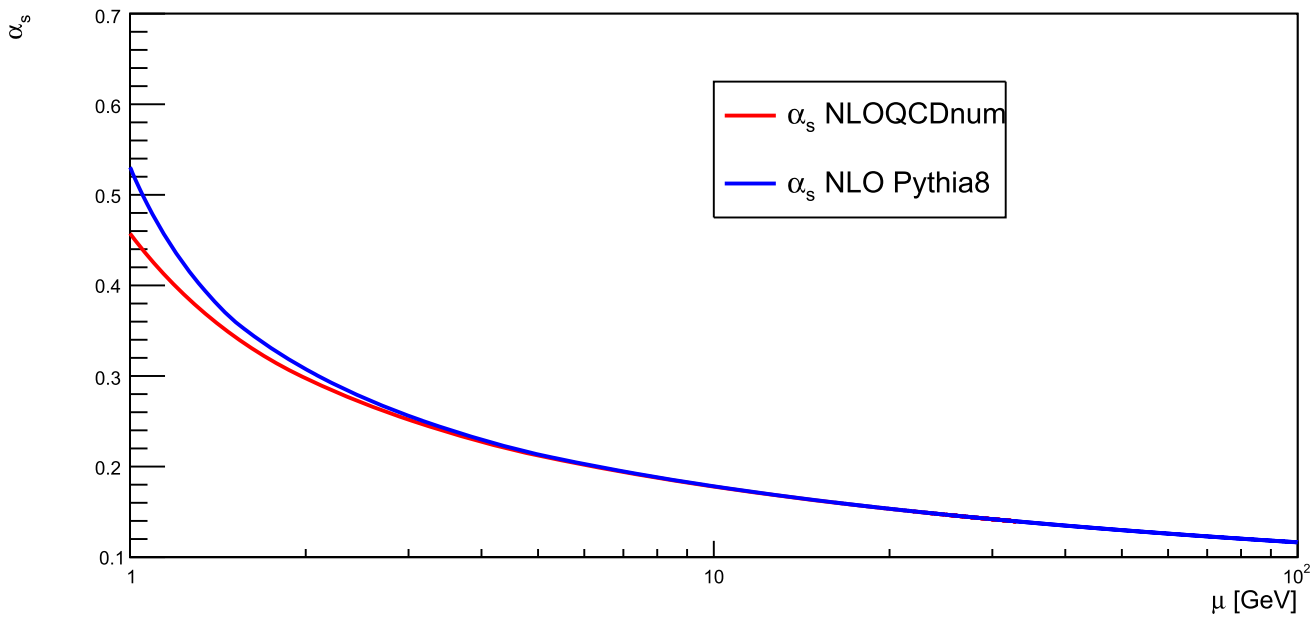

Fig. 6 The strong coupling as a function of the scale μ (with $\alpha_s(m_Z) = 0.118$) obtained from PYTHIA8 and QCDNUM

tions in the generation, but introducing an extra accept–reject step in the generation where an overall event weight is calculated from the ratio of NLO/LO as described in Refs. [16,17]. This ensures that the end result corresponds to using NLO both for the splitting functions and the Sudakov form factors. This procedure is described in more detail in Appendix A, and will produce fluctuating, and sometimes negative, event weights, which affect the statistical significance.

5.3 Full TMD distributions obtained with PDF2ISR at NLO

We are now in a position to compare the complete NLO distributions obtained from PYTHIA8PDF2ISR with the TMD distributions of PB-NLO-2018, which we used here as a test-case to show the consistency of the whole procedure. The method itself is universal, and can be also applied to any other collinear parton density at NLO.

Two things are worth noting here. The NLO splitting functions contain $1 \to 3$ type splittings that are integrated over, but the modified PYTHIA8 will emit only one parton, so only the (backward) evolution that is corrected to NLO, while the partons radiated into the final-state are still described correctly only at LO. This also means that it is straightforward also to go to NNLO evolution, keeping in mind that the final-state emissions are still at LO.

PB-NLO-2018 Set1 conditions In PB-NLO-2018 Set1 angular ordering is applied, but the scale in α_s is set to the evolution scale (as done in all DGLAP-based collinear parton densities). In Fig. 7, we compare PB-NLO-2018 Set1 distributions, calculated with NLO splitting functions and NLO α_s (as in Ref. [28]), to distributions obtained from the parton shower in PYTHIA8PDF2ISR, applying angular ordering and the PB Set1 conditions. Here, we set `pTmin=1.38` GeV, corresponding to the starting scale of $\mu_0 = 1.38$ GeV. For comparison, we also show predictions of PDF2ISR when only LO splitting functions are used for ISR. The distributions for the down quark and gluon are presented at different scales of $\mu = 10$ (100) GeV. The distributions agree very well if NLO splitting functions and consistent α_s values are used. Significant differences are observed, when only LO splitting functions are applied in the initial-state shower.

PB-NLO-2018 Set2 In PB-LO-2018 Set2, in addition to angular ordering, the scale in α_s is set as the transverse momentum of the emitted parton, defined with $q_t = (1-z)q'$. At large z, q_t can become very small, requiring special treatment for α_s at low scales; as in PB α_s is frozen at $q_{cut} = 1$ GeV. Details on how this is implemented in PYTHIA8PDF2ISR are provided in Appendix A.

Figure 8 shows distributions for down quark and gluon at various scales μ, applying PB-NLO-2018 Set2 at NLO. The blue curve shows the prediction using NLO splitting functions in PYTHIA8PDF2ISR together with the consistent α_s. The purple curve shows the prediction using the NLO calculation of α_s as calculated in PYTHIA8 which is different at small scales from the one used in PB-NLO-2018, as shown in Fig. 6. It is interesting to observe that a consistent treatment of α_s is required for a good description of the low k_t-part of the spectrum, especially for quarks. The agreement of the simulation PYTHIA8PDF2ISR with the calculation of PB-NLO-2018 Set2 at NLO for the quark channel is remarkable. The difference in the gluon channel arises from the use of different frame definitions when generating transverse momenta,

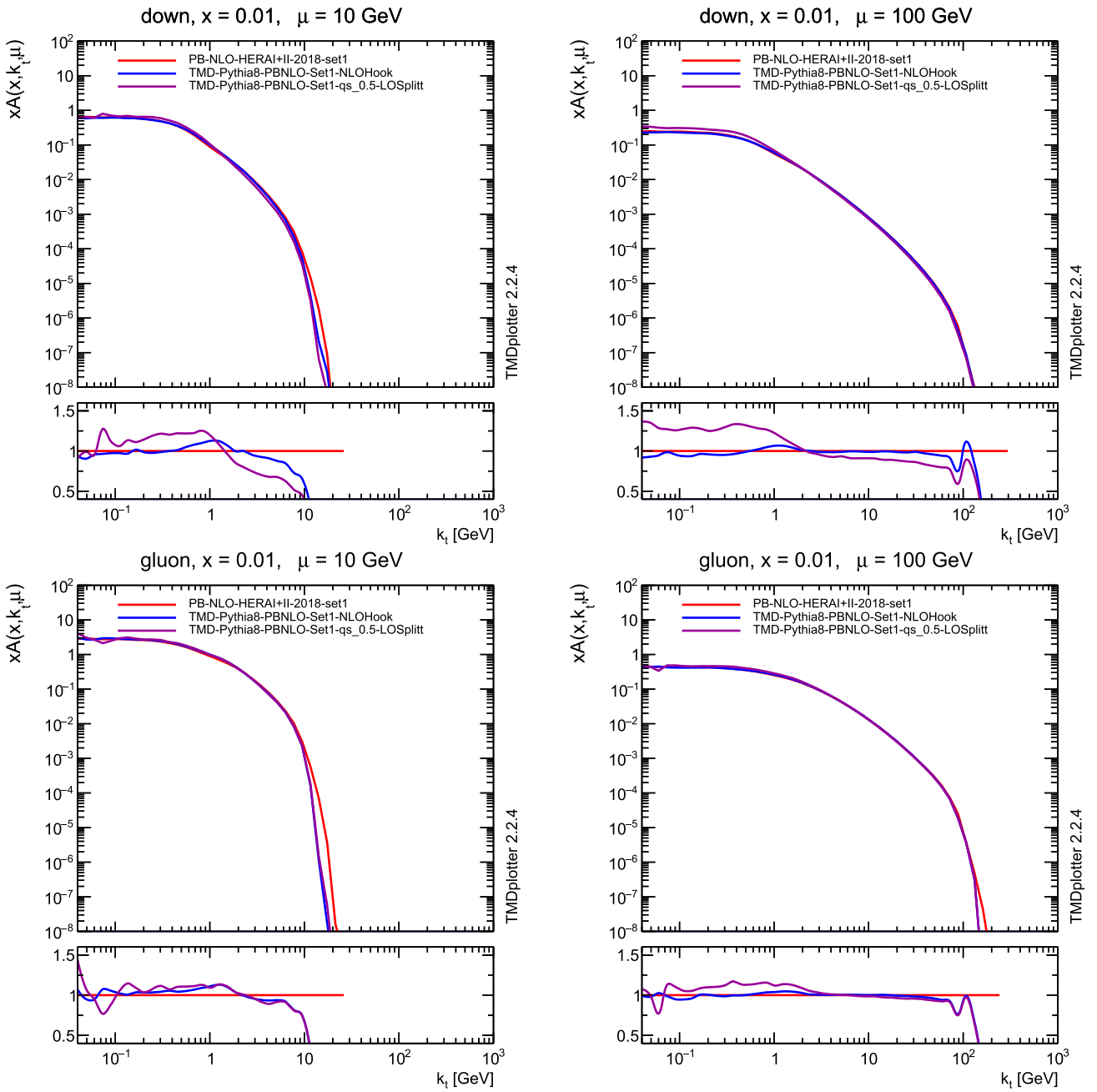

Fig. 7 Transverse momentum distributions for gluons and down-quarks as $\mu = 10(100)$ GeV, obtained from PB-NLO-2018 Set1 evolved from a starting scale $\mu_0 = 1.38$ GeV and PYTHIA8PDF2ISR applying `pTmin=1.38` GeV. The PB-NLO-2018 predictions are obtained at NLO (with NLO $\alpha_s(m_Z) = 0.118$ obtained from the parameterization in the LHApdf set). The blue line is obtained from PYTHIA8PDF2ISR with NLO splitting functions. The purple curve shows the prediction using LO splitting functions but still with NLO α_s

as discussed in detail in Appendix B, and can be treated as a systematic uncertainty related to the frame definition.

6 Conclusions

The main result of our study is that it is possible to construct an initial-state parton shower that is fully consistent with LO and NLO collinear parton densities.

In order to perform these studies, we have developed a method that allows us to construct Transverse Momentum Dependent parton densities from any parton shower event generator, a method we label as PS2TMD. The parton branching (PB) collinear and TMD parton densities were considered, since the TMDs provide a unique approach to study the parton branching processes in detail and in particular the effects from initial-state parton showers.

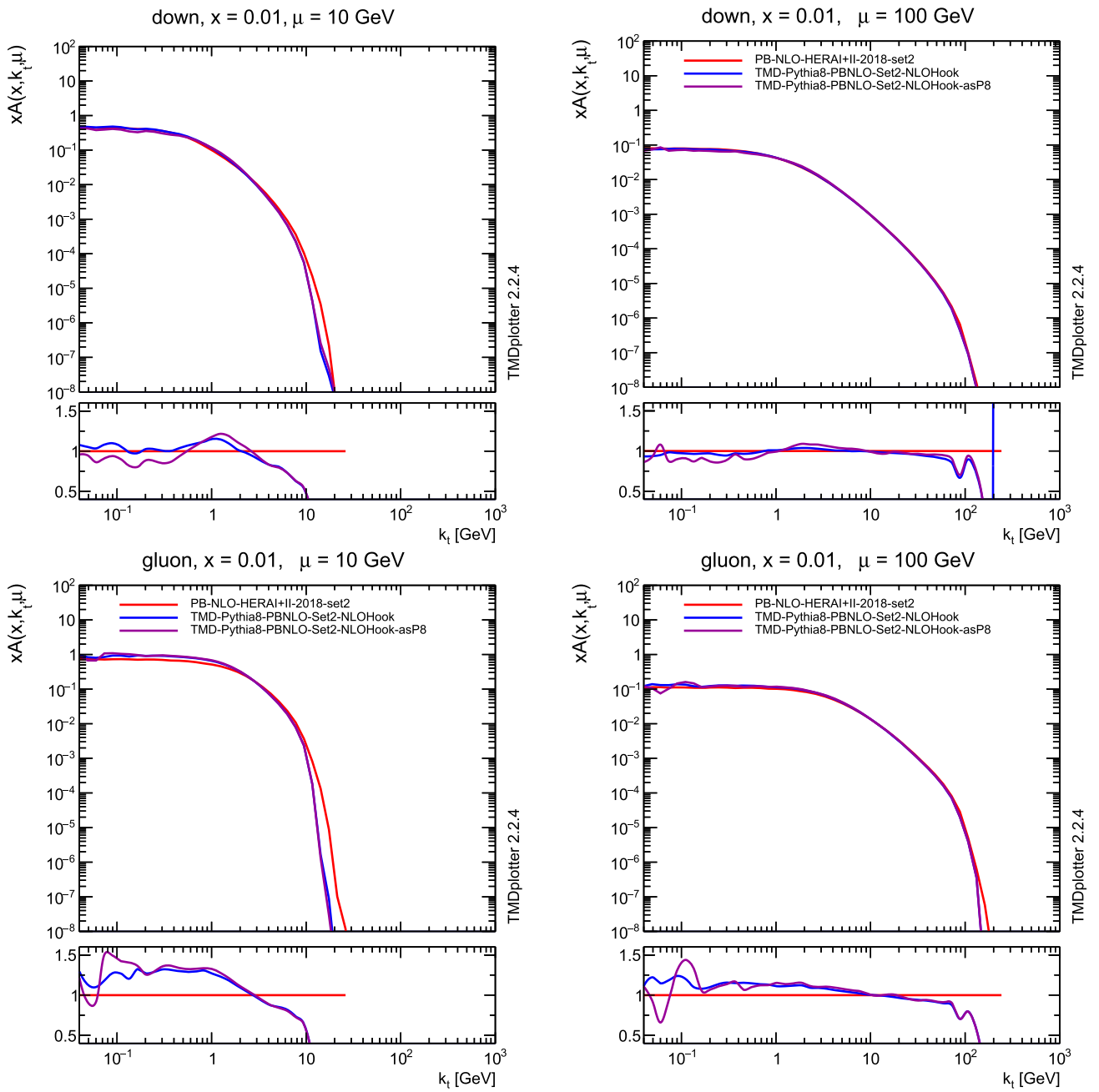

Fig. 8 Transverse momentum distributions for gluons and down-quarks as $\mu = 10(100)$ GeV, obtained from PB-NLO-2018 Set2 evolved from a starting scale $\mu_0 = 1.18$ GeV and PYTHIA8PDF2ISR applying `pTmin=1.18` GeV. The PB-NLO-2018 predictions are obtained at NLO (with NLO $\alpha_s(m_Z) = 0.118$). The blue line is obtained from PYTHIA8PDF2ISR with NLO splitting functions, the purple line shows the simulation when α_s as calculated rom PYTHIA8 is used, which is different at small scales from the one applied in PB-NLO-2018

We found that using LO parton densities and LO splitting functions within the parton shower leads to consistent results: the TMD distributions obtained by the PB-approach in a forward evolution are identical to those obtained from the backward evolution parton shower with PYTHIA8PDF2ISR, provided the same conditions are applied: angular ordering, kinematic limits, and the scale choice in α_s. This is already a big step forward in the understanding of parton showers and its relation to collinear parton densities.

A real breakthrough is acheived when considering TMD parton densities at NLO obtained with the PB-method. We could show that using NLO collinear parton densities but LO splitting functions within the parton shower leads to significant inconsistencies. Only by using the same evolution for α_s together with NLO splitting functions can consistent

results be achieved. In order to achieve this, we also had to deal with negative contributions from the splitting functions at large z (and small k_t). Applying a dedicated method of reweighting an oversampled parton shower allowed us to treat these effects correctly. We also showed that the definition of the frame of reference in which k_t is calculated matters; the frame is different in PYTHIA8PDF2ISR and UPDFEVOLV2.

The PDF2ISR method is universal and can be applied to any collinear parton density to obtain a consistent initial-state parton shower. The method is applicable at LO and NLO, as shown in this study, and can also be easily extended to NNLO.

Acknowledgements S. Taheri Monfared acknowledges the support of the German Research Foundation (DFG) under grant number 467467041.

Data Availability Statement My manuscript has no associated data. [Authors' comment: Data sharing not applicable to this article as no datasets were generated or analysed during the current study.]

Code Availability Statement My manuscript has no associated code/software. [Authors' comment: The Pdf2Isr code will be implemented as a plug-in to Pythia8, and can, in the meanwhile, be obtained upon request from the authors.]

Funded by SCOAP[3].

Appendices

A Modifying ordering in and splitting functions PYTHIA8

The PDF2ISR code will be implemented as a plug-in to PYTHIA8, and can, in the meanwhile, be obtained upon request from the authors. The changes we have made to the PYTHIA8 code are not substantial and are listed here for completeness.

A.1 The ordering

The backward evolution in the default initial-state parton shower, `SimpleSpaceShower`, in PYTHIA8, is ordered in transverse momentum, formally defined as (Ref. [2, p. 71])

$$q'^2 = p^2_{\perp\text{evol}} = (1-z)Q^2 - \frac{Q^4}{m^2_{ar}} \approx (1-z)Q^2 \tag{5}$$

where m^2_{ar} is the squared *dipole mass* of the two incoming partons on each side, which in our case is simply m^2_B in the first emission. The kinematics of the initial-state emissions are calculated from the z and Q^2 where $Q^2 = -(p_b - p_c)^2$ (using the notation in Fig. 1), so it is straightforward to reinterpret the evolution scale to be that of the angular scale $p_\perp/(1-z)$ in a few places.[6] and to modify the relationship between Q^2 and $p^2_{\perp\text{evol}}$ in the code,

$$Q^2 \approx p^2_{\perp\text{evol}}/(1-z) \quad \Rightarrow \quad Q^2 = (1-z)p^2_{\perp\text{evol}}. \tag{6}$$

The meaning of some parameters will change, e.g., the soft suppression and hard cutoff discussed in Sect. 3.3 will now refer to the angular variable rather than to the transverse momentum. So when we mention that we have set, e.g., `pTmin = 1.18`, it corresponds exactly to setting $\mu_0 = 1.18$ GeV in the TMD evolution.

A.2 NLO splitting functions and α_S

To modify the splitting functions and the α_S to conform to the NLO functions in QCDNUM we use the event reweighting technique in Ref. [16], implemented in a so-called `UserHooks` plug-in class to PYTHIA8. The plugin is accessed by PYTHIA8 after each initial-state emission, inside the Veto algorithm, and is asked whether the emission should be vetoed.

In our case we have artificially increased the fixed α_{S0} used in PYTHIA8 by a factor 2, and in the plug-in we then veto all emissions with a probability 0.5. This will give the same results as running without the plug-in but with an increased α_{S0}, except for an increase in running time. The trick is that we can now calculate an event weight, w_{ev}, that is used when filling histograms in Rivet, to reweight our LO results to give the desired NLO behaviour according to the following:

- For each suggested initial-state emission we calculate the NLO/LO ratios for the splitting functions and α_S:

$$r = \frac{P_{\text{NLO}}(z)}{P_{\text{LO}}(z)} \frac{\alpha_S^{\text{NLO}}(k^2_\perp)}{\alpha_{S0}} \tag{7}$$

- With probability 0.5 we will accept the emission, and update the event weight

$$w_{\text{ev}} \to w_{\text{ev}} \times r. \tag{8}$$

- If the emission is rejected, we instead update the event weight according to

$$w_{\text{ev}} \to w_{\text{ev}} \times (2-r). \tag{9}$$

[6] Inside the code, $p^2_{\perp\text{evol}}$ is given by the variable `pT2`.

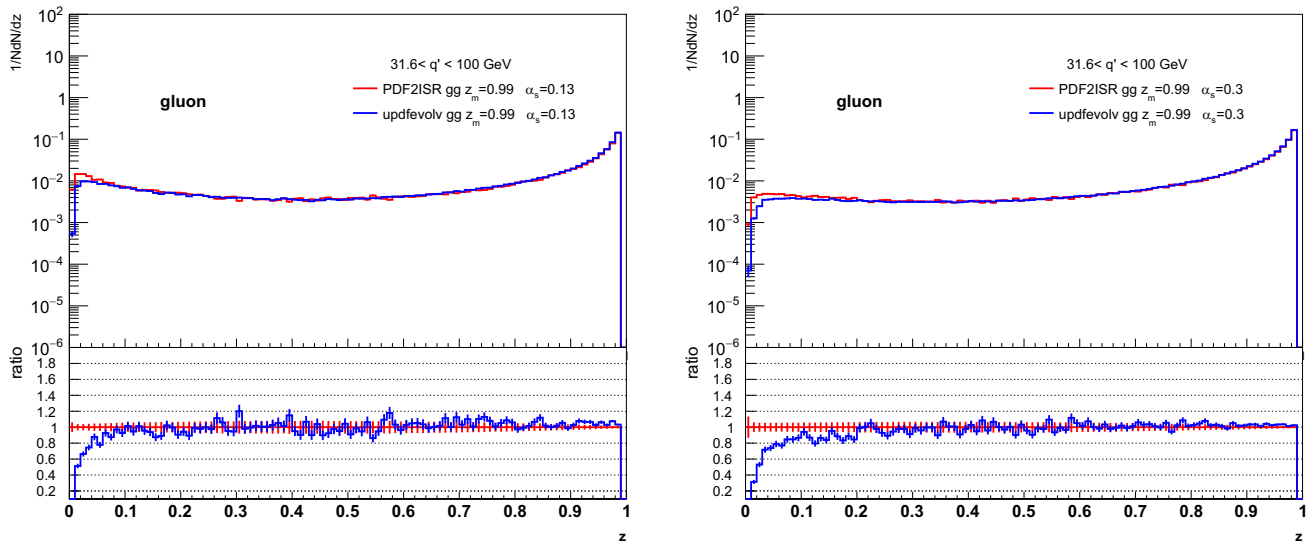

Fig. 9 Distribution of z for $g \to gg$ for $z_{\mathrm{M}} = 0.99$ and $31.6 < q' < 100$ GeV. The lower panel shows the ratio of the predictions from PYTHIA8 with the one from UPDFEVOLV2. Left: fixed $\alpha_s = 0.13$. Right: fixed $\alpha_s = 0.3$

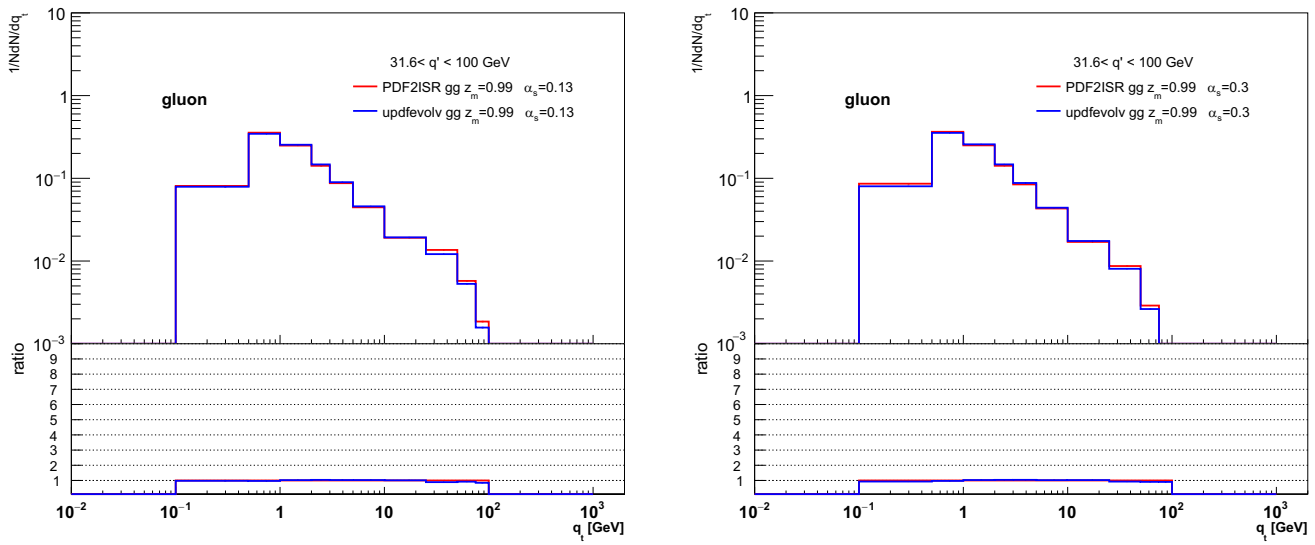

Fig. 10 Distribution of q_{t} for $g \to gg$ for $z_{\mathrm{M}} = 0.99$ and $31.6 < q' < 100$ GeV. The lower panel shows the ratio of the predictions from PYTHIA8 with the one from UPDFEVOLV2. Left: fixed $\alpha_s = 0.13$. Right: fixed $\alpha_s = 0.3$

In this way we reweight both the emission probability to get the correct NLO splitting, and the no-emission probability to get the correct NLO Sudakov form factor.

B Detailed comparison of forward and backward evolution

In the following, we perform a detailed comparison of the forward evolution, as used in UPDFEVOLV2, with the backward evolution implemented in the initial-state parton shower of PYTHIA8 with the PDF2ISR modifications described above. A simplified scenario is used, where only $g \to gg$ splittings are considered with the LO splitting function, a fixed cutoff $z_{\mathrm{M}} = 0.99$ and fixed α_s at $\alpha_s = 0.13\,(0.3)$. In the evolution, the scale q' is generated from the Sudakov form-factor Δ_{bw} (Eq. (4)), and the splitting variable is generated from the splitting function. The transverse momentum q_{t} of the emitted parton (see Fig. 1) is then calculated (assuming angular ordering) via $q_{\mathrm{t}} = q'(1 - z)$. In Fig. 9 the distribution of the splitting variable z is shown for a small slice of evolution scales $31.6 < q' < 100$ GeV. In Fig. 10 a comparison of q_{t} is shown. A rather good agreement between forward and backward evolution is observed.

The transverse momentum k_{t} (see Fig. 1) is calculated from q_{t}: in the forward evolution in UPDFEVOLV2 all cal-

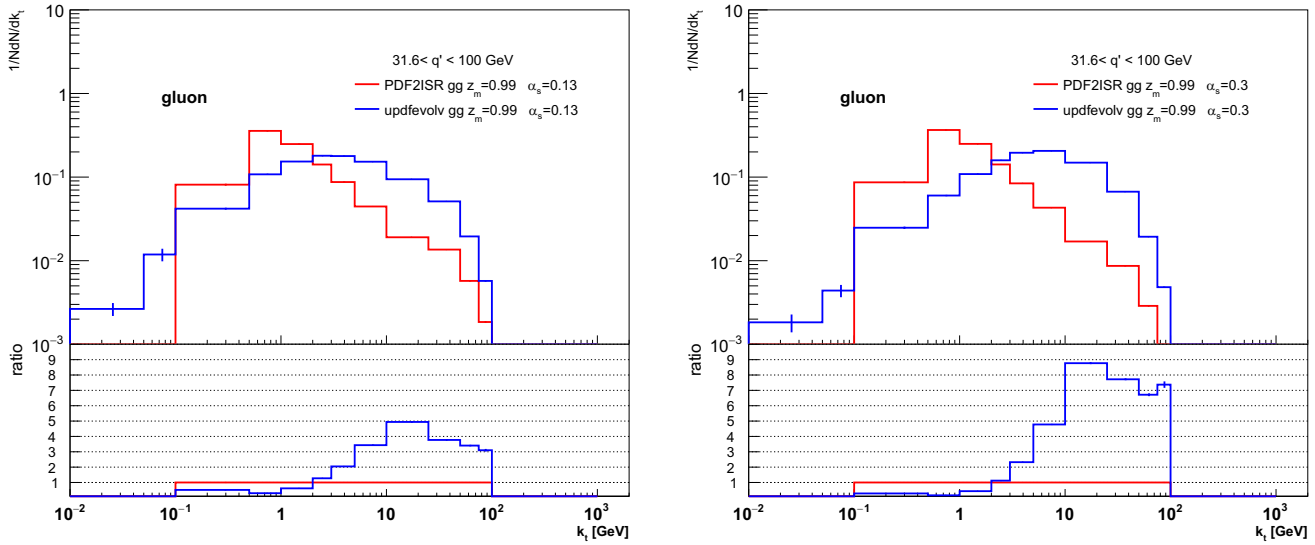

Fig. 11 Distribution of $k_t$for $g \to gg$ for $z_M = 0.99$. The lower panel shows the ratio of the predictions from PYTHIA8 with the one from UPDFEVOLV2. Left: fixed $\alpha_s = 0.13$. Right: fixed $\alpha_s = 0.3$

culations are performed in the overall center-of-mass frame, and the final k_t at the end of the evolution is given by [14,33]

$$\mathbf{k} = \mathbf{k}_0 - \sum_i \mathbf{q}_{t,i} \ . \tag{10}$$

where $\mathbf{k}_0$ comes from the intrinsic k_t-distribution (which is neglected here).

In the backward evolution in PYTHIA8, the transverse momentum q_t is defined in the collinear parton-parton center-of-mass frame, and the configuration is then boosted to the overall center-of-mass frame. The forward and backward evolution differ in the frame in which q_t is defined, and therefore differences are expected for k_t. In the case of large α_s, more emissions appear, and therefore a larger difference is expected. A comparison of the distributions of k_t for different α_s-values is shown in Fig. 11. One observes differences (significantly larger than for the q_t-distributions). The differences between backward and forward evolution are also significantly larger for $\alpha_s = 0.3$ compared to the case with $\alpha_s = 0.13$.

The differences observed in this simplified case help to explain the differences (especially in the gluon channel) observed for the Set2 scenario, where due to $\alpha_s(k_t)$, rather large values of α_s can be reached for small k_t (similar to the example above with fixed $\alpha_s = 0.3$).

The differences in the k_t-distribution, coming from the frame in which q_t is defined, can be associated as a systematic uncertainty, which, however, is covered already by a scale uncertainty of the TMD distribution. In Fig. 12, we show a comparison of the k_t-distribution obtained with the full forward evolution in UPDFEVOLV2 and the backward

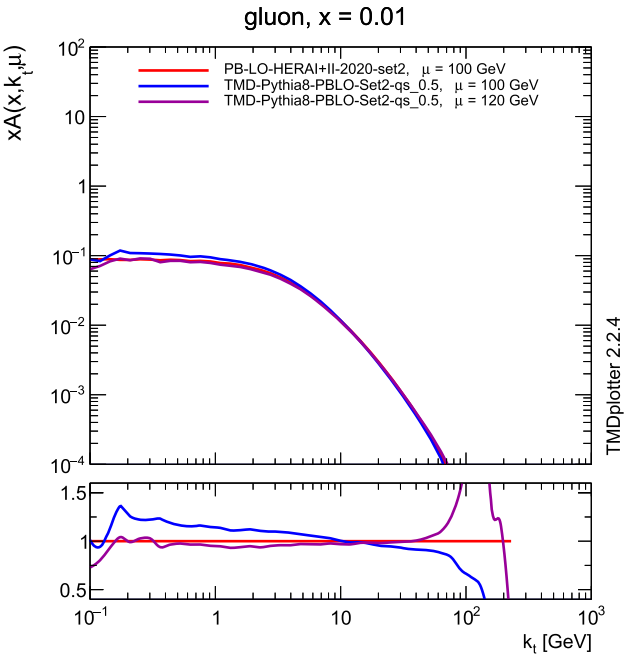

Fig. 12 Transverse momentum distributions for gluons at $\mu = 100$ GeV. The red line is from UPDFEVOLV2, the blue line is obtained from PYTHIA8PDF2ISR with LO splitting functions. The purple line shows the result with a slightly shifted scale $\mu = 120$ GeV

evolution in PYTHIA8. In addition is shown the prediction with a slightly shifted scale μ, showing that the differences are covered by a small variation of the scale μ.

C Parameter settings in PYTHIA8

Here, we give a full list of the parameters used in PYTHIA8. Note that setting `SpaceShower:PB` and the `Tune:pp` codes 100001–100004 are only available in our modifications of the code.

Settings for PB-NLO-2018 Set1

```
Tune:pp =                    100001
SpaceShower:PB =             1
PDF:pSet =
  LHAPDF6:PB-TMDNLO-HERAI+II-2018-set1
BeamRemnants:primordialKThard = 0.5
SpaceShower:alphaSvalue =    0.118
SpaceShower:alphaSorder =    2
SpaceShower:pT0Ref =         0.0
SpaceShower:pTmin =          1.38
SpaceShower:pTmaxFudge=      1.0
SpaceShower:rapidityOrder = false
SpaceShower:MEcorrections = false
SpaceShower:samePTasMPI =    false
1:m0 =                       0.
2:m0 =                       0.
3:m0 =                       0.
4:m0 =                       1.47
5:m0 =                       4.5
6:m0 =                       173.
```

Settings for PB-NLO-2018 Set2

```
Tune:pp =                    100002
SpaceShower:PB =             2
PDF:pSet =
  LHAPDF6:PB-TMDNLO-HERAI+II-2018-set2
BeamRemnants:primordialKThard = 0.5
SpaceShower:alphaSvalue =    0.118
SpaceShower:alphaSorder =    2
SpaceShower:pT0Ref =         0.0
SpaceShower:pTmin =          1.18
SpaceShower:pTmaxFudge =     1.0
SpaceShower:rapidityOrder = false
SpaceShower:MEcorrections = false
SpaceShower:samePTasMPI =    false
1:m0 =                       0.
2:m0 =                       0.
3:m0 =                       0.
4:m0 =                       1.47
5:m0 =                       4.5
6:m0 =                       173.
```

Settings for PB-LO-2018 Set1

```
Tune:pp =                    100003
SpaceShower:PB =             1
PDF:pSet =
  LHAPDF6:PB-TMDLO-HERAI+II-2018-set1
BeamRemnants:primordialKThard = 0.5
SpaceShower:alphaSvalue =    0.13
SpaceShower:alphaSorder =    1
SpaceShower:pT0Ref =         0.0
SpaceShower:pTmin =          1.38
SpaceShower:pTmaxFudge =     1.0
SpaceShower:rapidityOrder = false
SpaceShower:MEcorrections = false
SpaceShower:samePTasMPI =    false
1:m0 =                       0.
2:m0 =                       0.
3:m0 =                       0.
4:m0 =                       1.47
5:m0 =                       4.5
6:m0 =                       173.
```

Settings for PB-LO-2018 Set2

```
Tune:pp =                    100004
SpaceShower:PB =             2
PDF:pSet =
  LHAPDF6:PB-TMDLO-HERAI+II-2018-set2
BeamRemnants:primordialKThard = 0.5
SpaceShower:alphaSvalue =    0.13
SpaceShower:alphaSorder =    2
SpaceShower:pT0Ref =         0.0
SpaceShower:pTmin =          1.38
SpaceShower:pTmaxFudge =     1.0
SpaceShower:rapidityOrder = false
SpaceShower:MEcorrections = false
SpaceShower:samePTasMPI    = false
1:m0 =                       0.
2:m0 =                       0.
3:m0 =                       0.
4:m0 =                       1.47
5:m0 =                       4.5
6:m0 =                       173.
```

D TMDs for PB-LO-2018

The LO PB collinear and TMD sets PB-LO-2018 were obtained in Ref. [37], applying a starting scale $\mu_0 = 1.38$ GeVand $\alpha_s(m_Z) = 0.13$ (at LO).

In Fig. 13, the down quark and gluon distributions at LO obtained with PYTHIA8PDF2ISR applying `pTmin=1.38` GeV are shown and compared with those obtained with the LO PB- TMD distributions for Set1 conditions PB-LO-2018 Set1. A very good agreement is observed between the PB forward evolution and the PYTHIA8 parton shower in a backward evolution. The prediction without including intrinsic k_t is also shown for comparison.

A comparison of quark and gluon distributions of PB-LO-2018 Set2 obtained within the PB-approach with those from PYTHIA8PDF2ISR after applying the appropriate scale change in α_s is shown in Fig. 14 for different scales μ. Once again, a strong and satisfactory agreement is observed for the

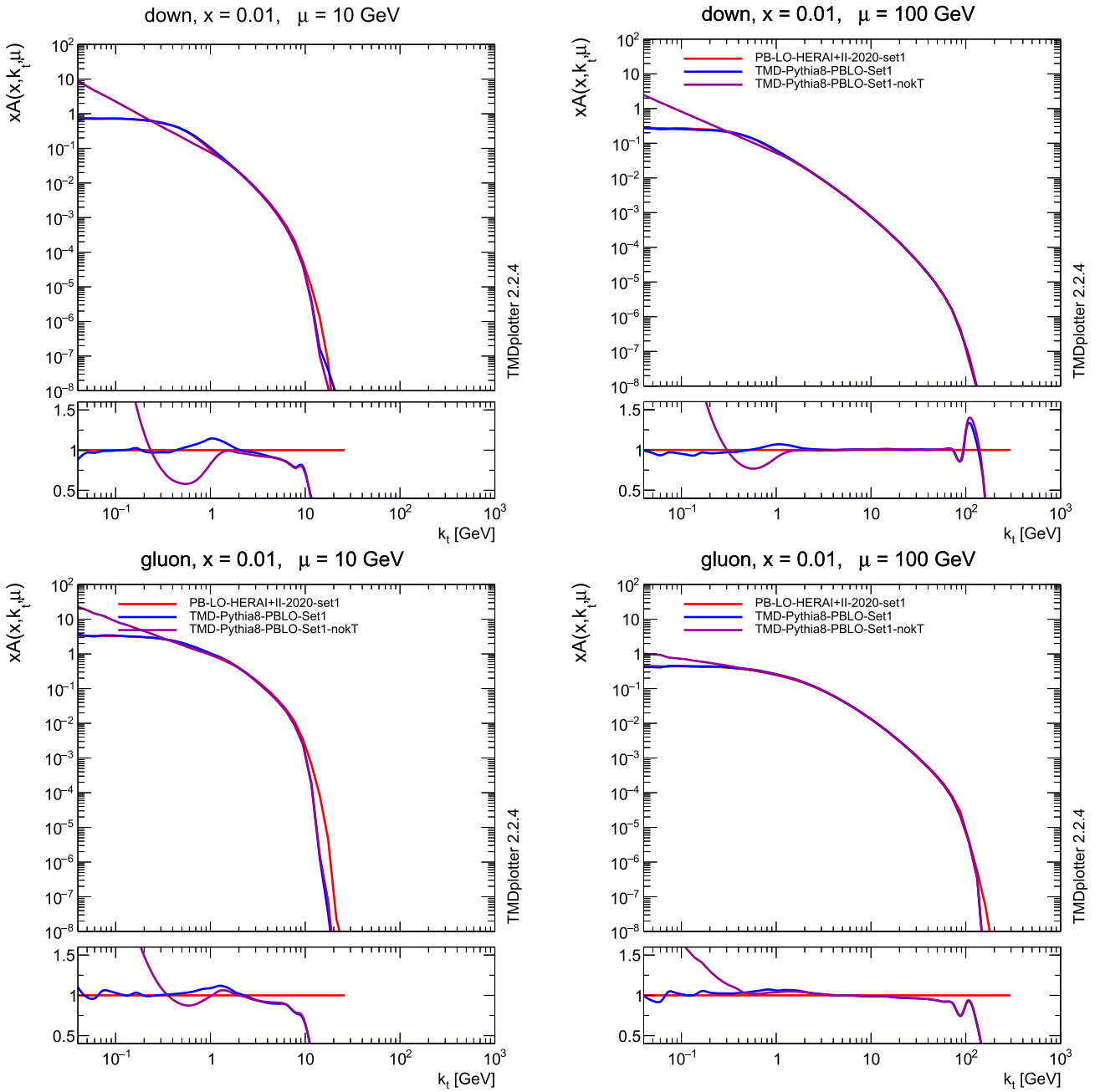

Fig. 13 Transverse momentum distributions for gluons and down-quarks as $\mu = 10(100)$ GeV, obtained from PB-LO-2018 Set1 evolved from a starting scale $\mu_0 = 1.38$ GeV and PYTHIA8PDF2ISR applying `pTmin=1.38` GeV. The PB-LO-2018 Set1 predictions are obtained at LO (with LO $\alpha_s(m_Z) = 0.130$)

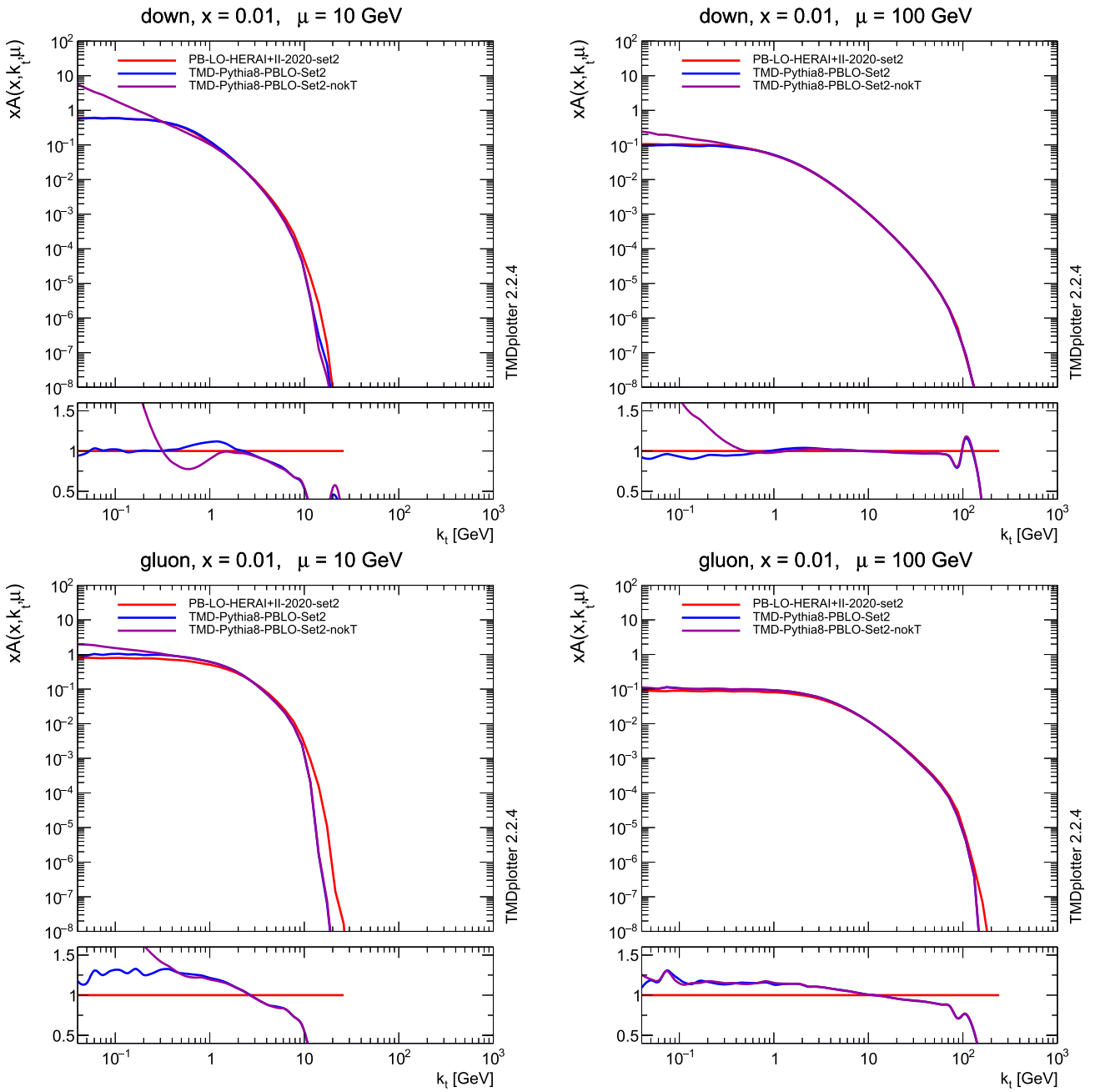

Fig. 14 Transverse momentum distributions for gluons and down-quarks as $\mu = 10$ (100) GeV, obtained from PB-LO-2018 Set2 evolved from a starting scale $\mu_0 = 1.38$ GeV and PYTHIA8PDF2ISR applying `pTmin=1.38` GeV. The PB-LO-2018 Set2 predictions are obtained at LO (with LO $\alpha_s(m_Z) = 0.130$)

quark distribution. The comparison of the gluon distribution is affected by the different reference frames as explained in Appendix B.

References

1. M. Bahr et al., Herwig++: physics and manual. Eur. Phys. J. C **58**, 639–707 (2008). arXiv:0803.0883
2. C. Bierlich et al., A comprehensive guide to the physics and usage of PYTHIA 8.3. SciPost Phys. Codeb. **2022**, 8 (2022). arXiv:2203.11601
3. S. Collaboration, Event generation with SHERPA 2.2. SciPost Phys. **7**(3), 034 (2019). arXiv:1905.09127
4. T. Gleisberg et al., Event generation with SHERPA 1.1. JHEP **0902**, 007 (2009). arXiv:0811.4622
5. J. Alwall et al., The automated computation of tree-level and next-to-leading order differential cross sections, and their matching to parton shower simulations. JHEP **1407**, 079 (2014). arXiv:1405.0301

6. C. Oleari, The POWHEG-BOX. Nucl. Phys. B, Proc. Suppl. **205**, 36 (2010). arXiv:1007.3893
7. S. Alioli, P. Nason, C. Oleari, E. Re, A general framework for implementing NLO calculations in shower Monte Carlo programs: the POWHEG BOX. JHEP **06**, 043 (2010). arXiv:1002.2581
8. S. Frixione, P. Nason, B.R. Webber, Matching NLO QCD and parton showers in heavy flavour production. JHEP **08**, 007 (2003). arXiv:hep-ph/0305252
9. S. Frixione, B.R. Webber, Matching NLO QCD computations and parton shower simulations. JHEP **06**, 029 (2002). arXiv:hep-ph/0204244
10. S. Frixione, P. Nason, C. Oleari, Matching NLO QCD computations with parton shower simulations: the POWHEG method. JHEP **0711**, 070 (2007). arXiv:0709.2092
11. P. Nason, B. Webber, Next-to-leading-order event generators. Annu. Rev. Nucl. Part. Sci. **62**, 187–213 (2012). arXiv:1202.1251
12. R. Frederix et al., A study of multi-jet production in association with an electroweak vector boson. JHEP **02**, 131 (2016). arXiv:1511.00847
13. S. Frixione, B.R. Webber, Correcting for cutoff dependence in backward evolution of QCD parton showers. JHEP **03**, 150 (2024). arXiv:2309.15587
14. F. Hautmann et al., Collinear and TMD quark and gluon densities from parton branching solution of QCD evolution equations. JHEP **01**, 070 (2018). arXiv:1708.03279
15. F. Hautmann et al., Soft-gluon resolution scale in QCD evolution equations. Phys. Lett. B **772**, 446 (2017). arXiv:1704.01757
16. S. Mrenna, P. Skands, Automated parton-shower variations in Pythia 8. Phys. Rev. D **94**, 074005 (2016). arXiv:1605.08352
17. L. Lönnblad, Fooling around with the Sudakov Veto Algorithm. Eur. Phys. J. C **73**, 2350 (2013). arXiv:1211.7204
18. H. Jung, S. Steel, S.T. Monfared, Y. Zhou, TMDs from Monte Carlo event generators. arXiv:2112.11248
19. M.V. Schmitz, Drell–Yan production with transverse momentum dependent parton densities. Master thesis, University of Hamburg, 2019. https://bib-pubdb1.desy.de/record/427383
20. C. Bierlich et al., Robust independent validation of experiment and theory: Rivet version 3. SciPost Phys. **8**, 026 (2020). arXiv:1912.05451
21. N.A. Abdulov et al., TMDlib2 and TMDplotter: a platform for 3D hadron structure studies. Eur. Phys. J. C **81**, 752 (2021). arXiv:2103.09741
22. S. Baranov et al., CASCADE3 A Monte Carlo event generator based on TMDs. Eur. Phys. J. C **81**, 425 (2021). arXiv:2101.10221
23. V.N. Gribov, L.N. Lipatov, Deep inelastic *ep* scattering in perturbation theory. Sov. J. Nucl. Phys. **15**, 438 (1972). [Yad. Fiz. 15, 781 (1972)]
24. L.N. Lipatov, The parton model and perturbation theory. Sov. J. Nucl. Phys. **20**, 94 (1975). [Yad. Fiz. 20, 181 (1974)]
25. G. Altarelli, G. Parisi, Asymptotic freedom in parton language. Nucl. Phys. B **126**, 298 (1977)
26. Y.L. Dokshitzer, Calculation of the structure functions for deep inelastic scattering and e^+e^- annihilation by perturbation theory in quantum chromodynamics. Sov. Phys. JETP **46**, 641 (1977). [Zh. Eksp. Teor. Fiz. 73, 1216 (1977)]
27. R.K. Ellis, W.J. Stirling, B.R. Webber, QCD and collider physics. Camb. Monogr. Part. Phys. Nucl. Phys. Cosmol. **8**, 1 (1996)
28. A. Bermudez Martinez et al., Collinear and TMD parton densities from fits to precision DIS measurements in the parton branching method. Phys. Rev. D **99**, 074008 (2019). arXiv:1804.11152
29. H1 and ZEUS Collaboration, Combination of measurements of inclusive deep inelastic $e^{\pm}p$ scattering cross sections and QCD analysis of HERA data. Eur. Phys. J. C **75**, 580 (2015). arXiv:1506.06042
30. M. Bengtsson, T. Sjostrand, M. van Zijl, Initial state radiation effects on W and jet production. Z. Phys. C **32**, 67 (1986)
31. M. Mendizabal, F. Guzman, H. Jung, S. Taheri Monfared, On the role of soft gluons in collinear parton densities. Eur. Phys. J. C **84**, 1299 (2024). arXiv:2309.11802
32. I. Bubanja et al., Center-of-mass energy dependence of intrinsic-k_{T} distributions obtained from Drell–Yan production. Eur. Phys. J. C **85**, 278 (2025). arXiv:2404.04088
33. H. Jung, A. Lelek, K.M. Figueroa, S. Taheri Monfared, The parton branching evolution package uPDFevolv2. arXiv:2405.20185
34. M. Botje, QCDNUM: fast QCD evolution and convolution. Comput. Phys. Commun. **182**, 490 (2011). arXiv:1005.1481
35. Particle Data Group Collaboration, Review of particle physics. J. Phys. G **33**, 1 (2006)
36. T. Sjöstrand, S. Mrenna, P. Skands, PYTHIA 6.4 physics and manual. JHEP **05**, 026 (2006). arXiv:hep-ph/0603175
37. H. Jung, S. Taheri Monfared, Collinear and TMD distributions from parton branching at LO. Private communication, PDF and TMD grid files can be obtained from the authors on request (2025)